VOL. 10, NO. 11, JUNE 2015 ISSN 1819-6608
ARPN Journal of Engineering and Applied Sciences
©2006-2015 Asian Research Publishing Network (ARPN). All rights reserved.
www.arpnjournals.com

# SOLAR POWERED BOOST CONVERTER FOR PMDC MOTOR DRIVEN ELECTRIC VEHICLE

ArunSrinivas T.[1], Rajendran V.[2]
[1]Department of Electrical & Electronics Engineering, Anna University, Chennai, India
[2]Department of Physics, SSN College of Engineering, Chennai, India
E-Mail: arunsrinivas1984@gmail.com

**ABSTRACT**

Electric cars which would dominate the future car industry would give off zero carbon emissions and are even better than hybrid vehicles in this regard because hybrids running on gas have emissions, while electric cars are totally 100 percent free of pollutants. An efficient DC/DC converter with soft switching topology is proposed in this paper to drive a permanent magnet DC motor that functions as the main thrust engine in the electric vehicle. This converter efficiently utilizes the energy stored in the inductors and capacitors to improve the performance of the Boost converter. With the interest in the utilization of renewable energy resources that is available in huge amount in India, the proposed converter is powered by the solar photovoltaic (PV) system. Power MOSFET that has the advantages of higher commutation speed, greater efficiency that can sustain a high blocking voltage and maintain a high current is used as a switching device in the chopper circuit. The speed control of the machine is achieved by using a simple pulse width modulation technique. The design and modelling of the proposed DC/DC converter is simulated by using MATLAB/SIMULINK tool and the results are analyzed and discussed in this paper.

**Keywords:** DC/DC boost converter, electric vehicle, PMDC, pulse width modulation.

## 1. INTRODUCTION

With the increasing demand for high voltage in the industrial applications, efficient DC/DC converter with high step up voltage gain is in high demand and is widely used. This need proliferates in designing an efficient DC/DC converter with reduced components, filter size and cost which will increase the marketability of the converter. Usually, the boost DC/DC converter operates at high step up voltage gain at high duty cycle. But unfortunately the passive elements present in the circuit become an obstacle for achieving high step up voltage gain. Hence in order to improve the efficiency of the converter, energy stored in the passive components like capacitor and the coupled inductor [1], [2] must be efficiently utilized by the system. Thus this paper proposes a transformer less high gain step up DC/DC converter [3] - [6] with practical and economical considerations.

Permanent Magnet DC (PMDC), [7] motors are widely used in a wide range of applications like battery powered electric vehicles, wheelchairs, conveyors, welding equipments and pumping equipments. Small electric vehicles like electric bicycles are used to carry and move light loads for a short distance. The application of electric vehicles has increased considerably in metros, especially in educational institutions and information technology parks in India. The PMDC motors are best suited for such applications as well as in heavy electric vehicles like formula race cars which require high starting torque, small size and energy efficient motors.

Solar irradiance (watt/$m^2$), temperature, insulation, angle of incident light, spectral characteristics of sunlight, dirt, shadow etc., are the main factors to be considered for the efficient operation of the solar cells. The PV cells are made up of silicon, which is also used in computer "chips". The radiation produced from the sun will be converted into direct current (DC) by the Photovoltaic process. The Maximum Power Point Tracking (MPPT) is the efficient way to track the maximum available output power of the PV system.

In operation, with a constant armature voltage, as speed decreases, available torque increases. Speed is controlled by varying the voltage applied to the armature. PMDC motors use a mechanical commutation scheme to switch current to the armature winding. Feedback devices sense motor speed and send this information to the control to vary its output voltage up or down to keep speed at or near the set value.

In Triangular PWM, the output voltage is controlled by varying the duty cycle. The duty cycle in turn is controlled by varying the reference and the carrier wave signals. In this method a constant reference signal $V_{ref}$ is compared with the triangular carrier wave signal. The peak magnitude is limited by the peak carrier wave signal.

Among all renewable energy sources, solar power systems [8] - [10] attract more attention because they provide excellent opportunity to generate electricity while greenhouse emissions are reduced. The only way of generating electricity from solar energy will be PV cells or panels. Many new MPPT algorithms have been proposed in various papers to improve the maximum power harvested from the solar panel. One such algorithm to improve the power output from a very low power (500mW) PV panel is attained by making use the controller as an external control loop of a plug and flow module collector chopper placed between the PV panel and the load [11].

©2006-2015 Asian Research Publishing Network (ARPN). All rights reserved.


## 2. MATERIALS AND METHODS IN THE PROPOSED CIRCUIT

### 2.1. Circuit Configuration

The circuit configuration of the proposed converter is shown in Figure-1.

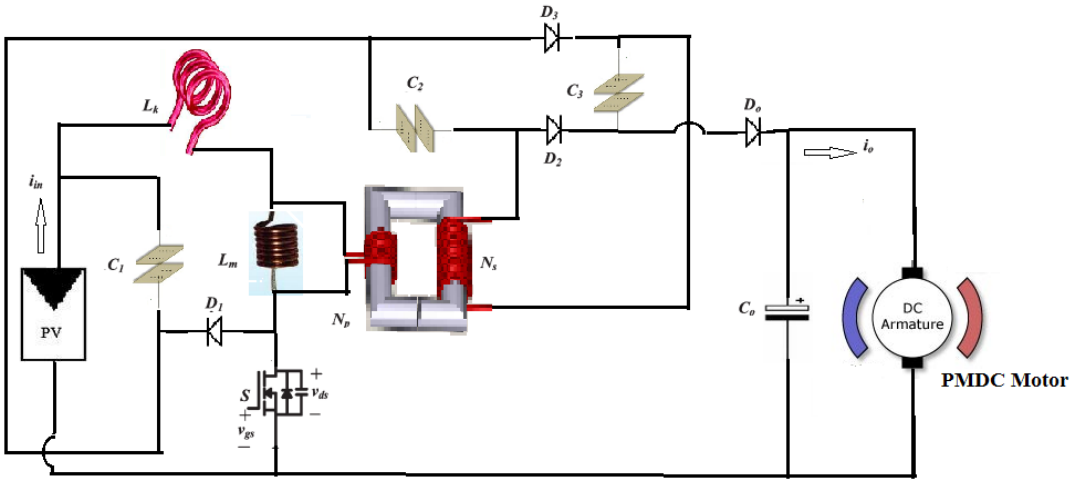


**Figure-1.** Circuit configuration of the proposed converter.

The main components of the proposed circuit are main switch S, clamping capacitor $C_1$, clamping diode $D_1$, one coupled inductor $N_p$ and Ns, two capacitors $C_2$ and $C_3$,two diodes $D_2$ and $D_3$, Output capacitor Co, and Output diode Do. This circuit is powered by a PV panel and it drives a PMDC motor load. The equivalent circuit model also includes leakage inductance $L_k$ and magnetizing inductance $L_M$.

The leakage energy stored in the coupled inductor is recycled to the capacitor and hence the voltage stress across the switch is reduced. This feature of the proposed converter increases the perfornance and thus the efficiency of the converter.

### 2.2.Operating principle of the proposed converter

When switch is ON, Vin charges $L_M$ and in turn the secondary side of the coupled inductor. Similarly, when the switch is OFF, the energy stored in $L_M$ is discharged through the secondary side of the coupled inductor. Inorder to reduce the voltage across the switch S, the capacitors $C_2$ aand $C_3$ discharges in series whereas they charge in parallel during the turn OFF and turn ON process respectively.

### 2.3.Continuous current mode operation of the proposed converter

There are five operating modes in each switching cycle. Each operating mode is discussed below in detail.

**Mode I:** In this mode, S is ON. As mentioned in the previous topic,Vin charges $L_M$ and the secondary side of the coupled inductor. Thus the secondary side current $i_s$ charges $C_2$ and turns ON the diodes $D_2$, $D_3$ and the capacitor $C_3$. The output capacitor Co supplies the load. The current flow is shown in Figure-2(a). The expression for the input voltage can be written as,

$$V_{in} = VL_K + VL_M \quad (1)$$

**Mode II:** During this interval, S remains ON, the source current charges $L_M$ and also travels to the secondary side through the coupled inductor. A part of the surce current takes the path of capacitors $C_1$, $C_2$ and $C_3$. All the three capacitors discharge the stored energy in series to the load by turning ON the output diode Do. Figure-2(b)shows the current flow direction.

**Mode III:** As soon as, the three capacitors completely discharge to the output voltage, S is turned OFF. The source current thus flows through the coupled inductor, $L_M$, and the parasitic capacitor $C_{ds}$ of the switch S. Thus ZVS is achieved for the switch S. The output capacitor Co supplies the load. Figure-2(c)represents this mode.

**Mode IV:** In this mode, the moment the parasitic capacitor $C_{ds}$ gets fully charged, the source current now flows through the $L_M$, coupled inductor, $D_1$, $C_2$,$C_3$,$D_o$ and the load. Further the energy stored in the leakage inductor $L_k$ is recycled through the clamping capacitor C1. The circuit representation for the above explanation is shown in Figure-2(d).

**Mode V:** During this interval, the supply voltage is detached. The recycled energy of $L_k$ flows through $L_M$. The current flowing through also flows through the coupled inductor. This charges the capacitors $C_2$ and $C_3$ in parallel. The secondary current also flows through the diodes D2 and D3. $C_o$ supplies the load. At the end of this mode switch S turns ON and the cycle continues. Figure-2(e) shows the circuit diagram representation of this mode.

©2006-2015 Asian Research Publishing Network (ARPN). All rights reserved.


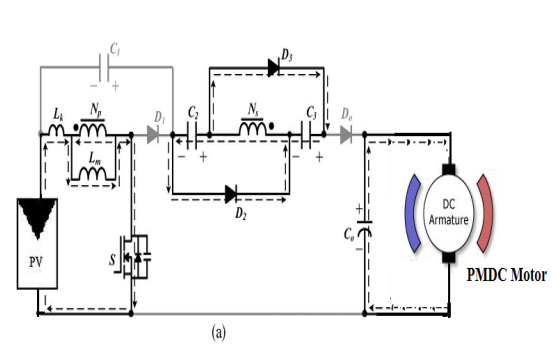


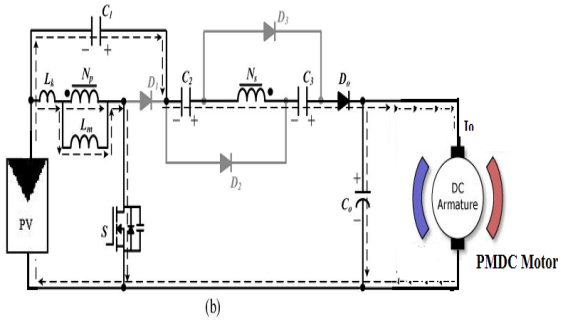


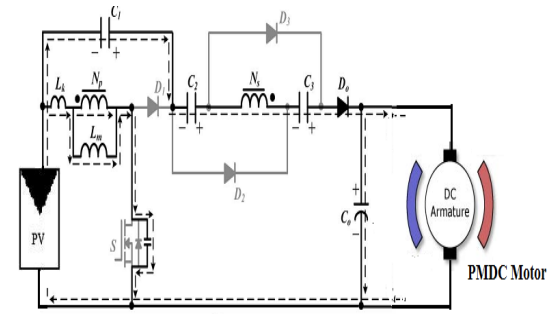


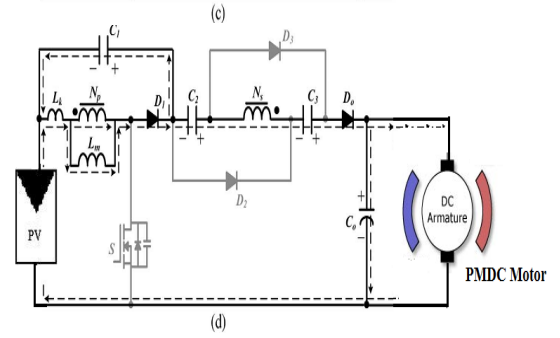


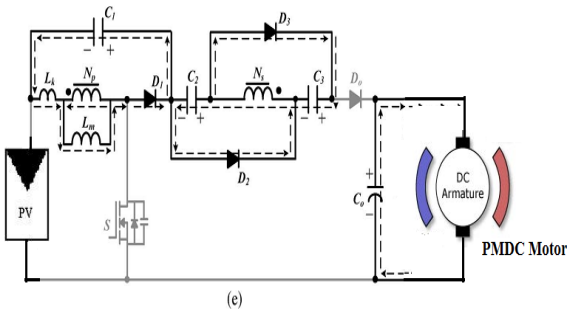


**Figure-2.** Modes of operation of the proposed converter.

## 3. MODELING OF MOTOR AND SOURCE

### 3.1. Modeling of permanent magnet DC motor

The PMDC machine used for practical application has a rated speed of 3500rpm. The following are the guiding equations of a PMDC motor.

$$V = (Ia \times Ra) + Eb \quad (2)$$

$$E_b = k \times \omega \quad (3)$$

$$\omega = 2 \times \pi \times N \quad (4)$$

$$\text{Generated Torque, } T_e = kxI \text{ Nm} \quad (5)$$

where,

$E_b$ =Back EMF in volts
$\omega$ = Angular speed in rad/sec.
N = Speed in rpm

Factor k depends on motor design features (number of winding turns, permanent magnet strength, air gap distance, rotor diameter, rotor length). The PMDC motor directly provides rotary motion and, coupled with wheels or drums and cables, can provide transitional motion. The electric circuit of the armature and the free body diagram of the rotor are shown in the Figure-3.

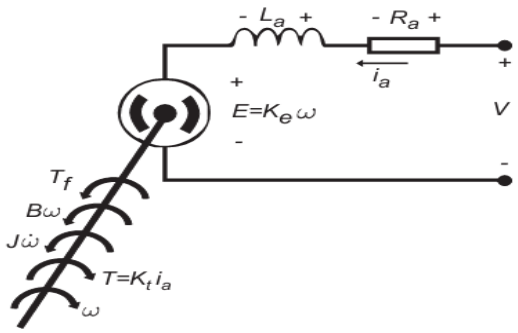


**Figure-3.**Circuit model of PMDC motor.

©2006-2015 Asian Research Publishing Network (ARPN). All rights reserved.


The motor torque, T, is related to the armature current, ia, by a constant factor $K_t$. The back emf, E, is related to the rotational velocity by the constant factor $K_e$ as in the following equations:

$$T = K_t . i_a \quad (6)$$

$$E = K_e . \omega \quad (7)$$

$$V = R_a . i_a + L_a \frac{di_a}{dt} + K_e \omega \quad (8)$$

$$K_t i_a = J\frac{d\omega}{dt} + B_m \omega + T \quad (9)$$

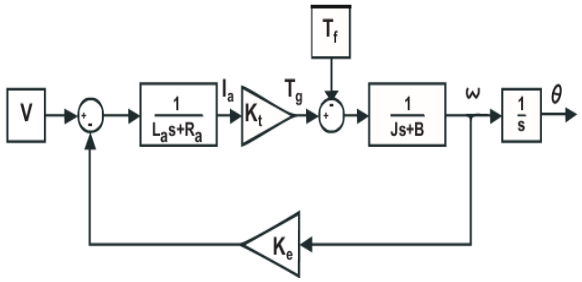


**Figure-4.**Modelling of PMDC motor.

The modeling of the PMDC motor is drawn using the above equations as shown in Figure-4.

### 3.2 Modeling of photovoltaic array system

The PV panel module physically moves to point directly at the sun and which the MPPT is not a mechanical tracking system. The battery is directly connected to the module and it is charging a discharged battery. Hence the module will be operated at battery voltage. The equivalent circuit of the PV cell in shown in Figure-5.

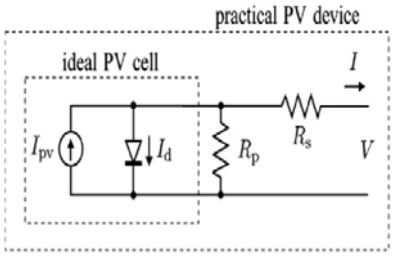


**Figure-5.**Equivalent circuit of PV cell.

The basic equation of I - V characteristic of the ideal PV is mathematically described from the theory of semiconductors

$$I = I_{pv,cell} - I_d \quad (10)$$

$$I_d = I_{o,cell} [\exp (qv/\alpha kt)] - 1] \quad (11)$$

therefore,

$$I = I_{pv,cell} - I_{o,cell}[\exp (qv/\alpha kt)] - 1] \quad (12)$$

where,

- $I_{pv,cell}$ is the current generated by the incident light (it is directly proportional to the Sun irradiation),
- $I_d$ is the Shockley diode equation,
- $I_{0,cell}$ is the reverse saturation or leakage current of the diode, *q* is the electron charge ($1.6 \times 10^{-19}$ C),
- *k* is the Boltzmann constant ($1.38 \times 10^{-23}$ J/K), *T* (in Kelvin) is the temperature of the *p–n* junction, and *a* is the diode ideality constant.

The Figure-6 shows the origination of the I–V curve for the equation (12).

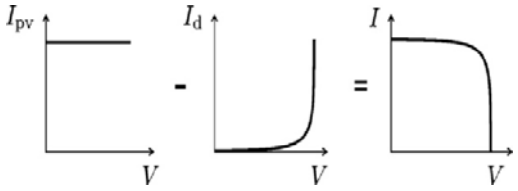


**Figure-6.**Origin of I-V equation of an Ideal PV cell.

Practical arrays are made up of multiple modules. The observation of the characteristics at the terminals of the PV array requires the inclusion of additional parameters to the basic equation.

$$I = I_{pv} - I_o[\exp (V + RsI)/Vt \alpha) - 1] - (V + RsI)/Rp) \quad (13)$$

where,$V = N_s kT/q$ is the thermal voltage of the array with $N_s$ cells connected in series.$R_S$and $R_P$are the equivalent series and parallel resistance of the array. The cells connected in parallel which increases the current and the greater output voltage will be produced by the cells connected in series. The $N_p$ parallel connections of cell composes the array, the PV and saturation currents may be expressed as,

$$I_{pv} = {}_{Ipv,cell} * N_p \quad (14)$$

$$I_o = I_{o,cell} * N_p \quad (15)$$

### 3.3. Design of circuit parameters

The circuit parameters are designed based on the load parameters mentioned in Table-1.

©2006-2015 Asian Research Publishing Network (ARPN). All rights reserved.


**Table-1.** Motor parameters.

| Parameters | Values |
|---|---|
| Armature voltage ($V_a$) | 100V |
| Aramture current ($I_a$) | 5.2A |
| Armature resistance ($r_a$) | 20 Ω |
| Aramture inductance ($L_{AA}$) | 1.6 mH |
| Moment of Inertia (J) | 1.06 x $10^{-6}$ Kg $m^2$ |
| Viscous friction co-efficient ($B_m$) | 3.79 x $10^{-3}$ Nms/rad |
| Constant ($k_v$) | 0.52 |
| Full load torque ($T_L$) | 2.7 Nm |

$$L_m = f_s \cdot \frac{D^3 - 2D^2 + D}{R_q\ 2n^2 + 4n + 2} = 48\mu F \quad (16)$$

$$V_{DS} = V_{D1} = \frac{V_{in}}{1 - D} = 24V \quad (17)$$

$$V_{D2} = V_{D3} = V_{Do} = \frac{nV_{in}}{1 - D} = 96V \quad (18)$$

Where

D = Duty cycle (here duty cycle is considered as 50%)
Lm = Magnetizing inductance

The magnitude of the dc modulating signal is constrained to remain between the minimum and maximum magnitudes of the triangular carrier signal. Now, the high frequency triangular carrier waveform is compared with the dc modulating signal and the comparator output is used to control the switch.

## 4. DISCUSSIONS OF SIMULATION RESULTS

The performance of the proposed converter is illustrated using PMDC motor load. The performance is studied by using Matlab simulation. The simulink model of the proposed converter with the PMDC motor load is shown in Figure-7. The input voltage, input current and the pulse pattern are shown in Figure-8, 9 and 10, respectively.

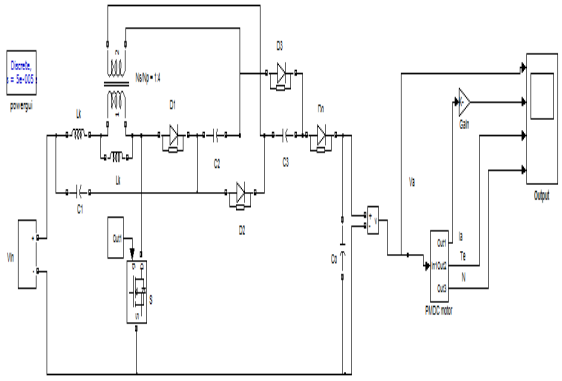

**Figure-7.** Simulink model of the proposed circuit.

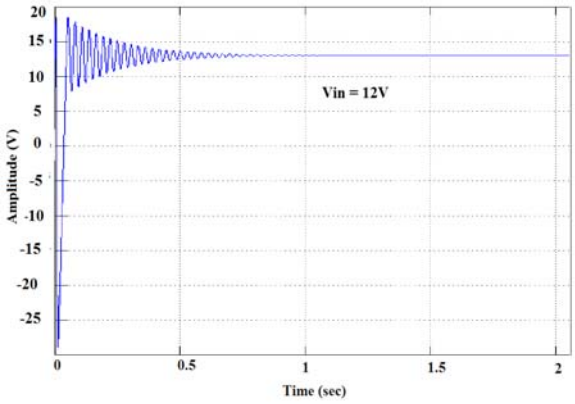


**Figure-8.** Input voltage vs time.

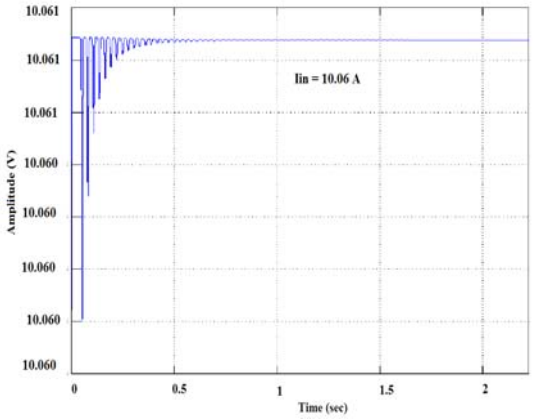


**Figure-9.** Input current vs time.

©2006-2015 Asian Research Publishing Network (ARPN). All rights reserved.


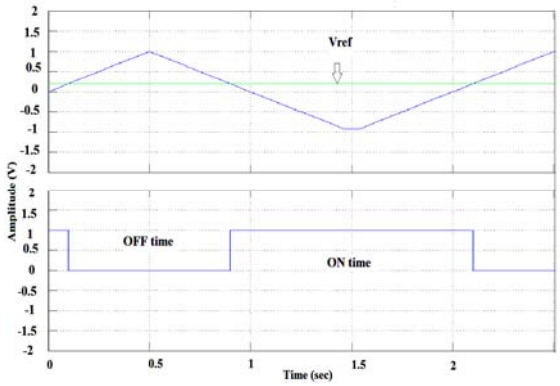


**Figure-10.**Pulse generation using triangular pulse width modulation.

The resultant armature voltage, armature current, motor speed and torque is shown if figures 11,12, 13 and 14,respectively. Pulses for the gate terminal of the power semiconductor device are generated using triangular pulse width modulation (PWM) technique as shown in Figure-10.A 0.5HP, 1640rpm PMDC motor is driven by using a 12V solar panel. The armature voltage and the armature current obtained from this proposed system are 100V and 5A, respectively.

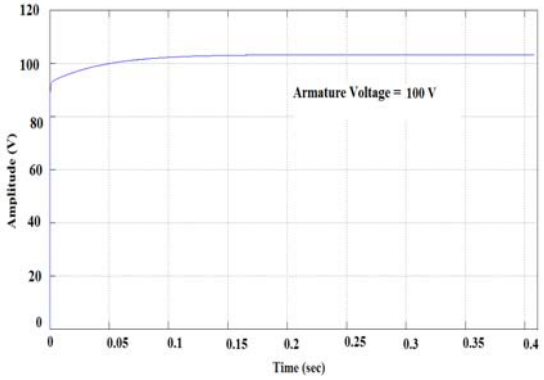


**Figure-11.**Armature voltage vs time.

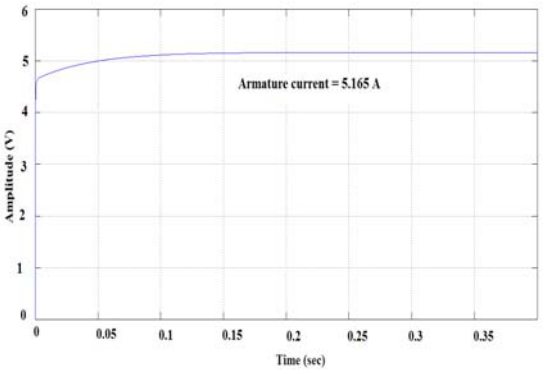


**Figure-12.**Armature currentvstime.

The variation of the speed of the BLDC machine with respect to the variation of the output voltage of the chopper is tabulated in Table-2 and it is verified that the motor speed increases with increase in chopper output voltage.

**Table-2.**Chopper voltage vs BLDC motor speed.

| **Input voltage** (V) | **Speed** (rpm) |
|---|---|
| 12 | 1640 |
| 24 | 2046 |
| 36 | 2198 |
| 48 | 3069 |

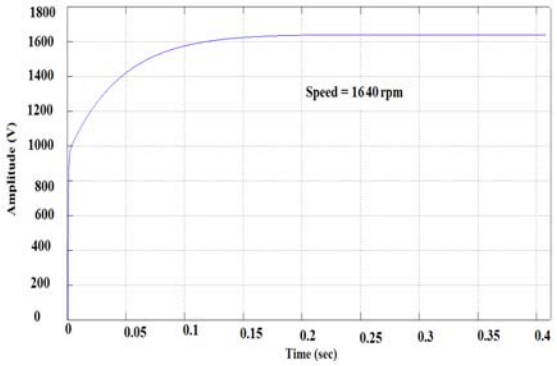


**Figure-13.**Motor speed vs time.

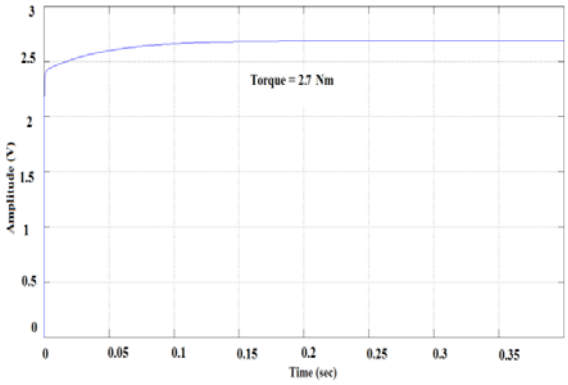


**Figure-14.**Motor torque vs time.

## 5. DISCUSSION OF HARDWARE RESULTS

The proposed simulated work has been implemented in hardware using a prototype model consisting of a PV panel. The input terminal is connected to the ZVS boost DC-DC converter as shown in the Figure-15. The proposed converter system is powered by a 12V solar PV panel. The output of the converter drives a High speed PMDC motor load. The output boost Voltage waveform of the ZVS is given in the Figure-18.

©2006-2015 Asian Research Publishing Network (ARPN). All rights reserved.


The specifications are as follows:

a) Solar panel output $V_{in}$: 12V

b) Output dc voltage $V_o$: 100 V

c) Motor output power: 0.5 HP

d) Switching frequency: 50 kHz

e) MOSFETS: IRFB4410ZPBF

f) Diodes D1: SBR20A100CTFP, $D_2$& $D_3$: DESI30, and $D_o$: BYR29

g) Coupled inductor: ETD-59, core pc40, $N_p$: $N_s$=1:4,$L_m$=48µH, and $L_k$=0.25µH

h) Capacitors $C_1$:56µF /100 V, $C_2$and $C_3$:22µF/200 V, and $C_o$: 180µF /450 V.

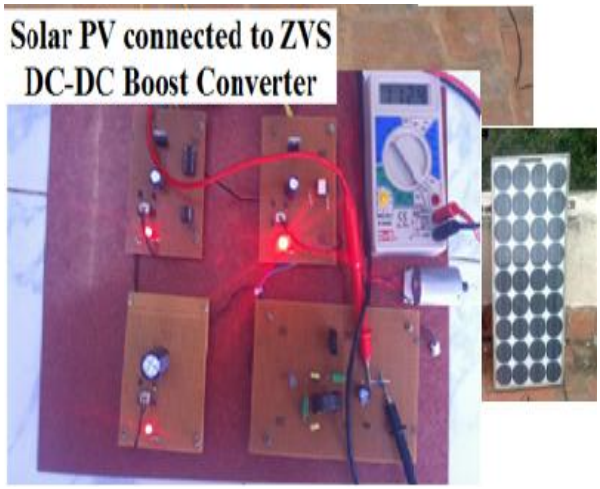


**Figure-15.**Hardware setup of the proposed system.


**Figure-16.**Switching pulse of the chopper controller circuit.


**Figure-17.**Switching pulse of driver circuit.


**Figure-18.**Waveform of output voltage.

## 6. CONCLUSIONS

The performance of the DC/DC converter is improved in this paper by effectively utilizing the energy stored in the passive elements. This converter is powered by the renewable of energy i.e. solar. The proposed system can be efficiently utilized in high speed drive applications. In this case, the proposed system is made to drive a PMDC motor load. The converter receives an input voltage of 12V from the solar panel, and in turn produces 100V/ 5A driving a PMDC motor load of 0.5 rating. Further, soft switching technique with Triangular pulse width modulation strategy reduces the switching losses and stress thereby improving the efficiency further. Moreover as the energy stored in the passive elements is effectively utilized, the overall losses reduce considerably there adding the efficiency percentage. And also this proposed system is cost effective and can be used in wide range of drive applications.

©2006-2015 Asian Research Publishing Network (ARPN). All rights reserved.


**ACKNOWLEDGEMENT**

The authors would like to thank the Management of Jeppiaar Engineering College and SSN College of Engineering, Chennai, India for providing the facilities to carry out this research.

**REFERENCES**

[1] T. F. Wu, Y. S. Lai, J. C. Hung, and Y. M. Chen. 2008. Boost converter with coupled inductors and buck–boost type of active clamp. IEEE Transactions on Industrial Electronics. 55(1): 154-162.

[2] R. J. Wai and R. Y. Duan. 2005. High step-up converter with coupled-inductor. IEEE Transactions on Power Electronics. 20(5): 1025-1035.

[3] L. S. Yang, T. J. Liang, and J. F. Chen. 2009. Transformerless dc-dc converter with high voltage gain. IEEE Transactions on Industrial Electronics. 56(8): 3144-3152.

[4] N. P. Papanikolaou and 4. E. C. Tatakis. 2004. Active voltage clamp in fly back converters operating in CCM mode under wide load variation. IEEE Transactions on Industrial Electronics. 51(3): 632-640.

[5] R. J. Wai and R. Y. Duan. 2005. High-efficiency dc/dc converter with high voltage gain.In Proceedings of IET-Electric Power Appications. 152(4): 793-802.

[6] Q. Zhao and F. C. Lee. 2003. High-efficiency, high step-up dc–dc converters. IEEE Transactions on Power Electronics. 18(1): 65-73.

[7] O. Abutbul, A. Gherlitz, Y. Berkovich and A. Ioinovici. 2003. Step-up switching-mode converter with high voltage gain using a switched-capacitor circuit. IEEE Transactions on Circuits and Systems I: Fundamental Theory Applications. 50(8): 1098-1102.

[8] M. G. Guerreiro, D. Foito and A. Cordeiro. 2013. A Sensorless PMDC Motor Speed Controller with a Logical Overcurrent Protection. Journal of Power Electronics. 13(3).

[9] Nobuyoshi Mutoh, Masahiro Ohno and Takayoshi Inoue. 2006. A Method for MPPT Control While searching for Parameters Corresponding to Weather Conditions for PV Generation Systems. IEEE Transactions on Industrial Electronics. 53(4).

[10] Nicola Femia, Giovanni Petrone, Giovanni Spagnuoloand Massimo Vitelli. 2005. Optimization of Perturb and Observe Maximum Power Point Tracking Method.IEEE Transactions on Power Electronics. 20(4).

[11] Oscar López-Lapeña, Maria Teresa Penellaand Manel Gasulla. 2005. A New MPPT Method for Low-Power Solar Energy Harvesting.IEEE Transactions onIndustrial Electronics. 57(9).